doi:10.1016/j.jmb.2003.12.005 J. Mol. Biol. (2004) 336, 187–196

JMB

Available online at www.sciencedirect.com

SCIENCE DIRECT®

ELSEVIER

Structural Distortion of p53 by the Mutation R249S and its Rescue by a Designed Peptide: Implications for "Mutant Conformation"

Assaf Friedler, Brian S. DeDecker, Stefan M. V. Freund, Caroline Blair Stefan Rüdiger and Alan R. Fersht*

Cambridge University Chemical Laboratory and Cambridge Centre for Protein Engineering, MRC Centre Hills Road, Cambridge CB2 2QH, UK

Missense mutations in the DNA-binding core domain of the tumour suppressor protein p53 are frequent in cancer. Many of them result in loss of native structure. The mutation R249S is one of the six most common cancer-associated p53 mutations ("hot-spots"). As it is highly frequent in hepatocellular carcinoma, its rescue is an important therapeutic target. We have used NMR techniques to study the structural effects of the R249S mutation. The overall fold of the core domain is retained in R249S, and it does not take up a denatured "mutant conformation". However, the β-sandwich had increased flexibility and, according to changes in chemical shift, there was local distortion throughout the DNA-binding interface. It is likely that the R249S mutation resulted in an ensemble of native and native-like conformations in a dynamic equilibrium. The peptide FL-CDB3 that was designed to rescue mutants of p53 by binding specifically to its native structure was found to revert the chemical shifts of R249S back towards the wild-type values and so reverse the structural effects of mutation. We discuss the implications for a rescue strategy and also for the analysis of antibody-binding data.

*Corresponding author

Keywords: p53; mutant; cancer; NMR; peptide

Introduction

The tumour suppressor p53 is at the centre of the cellular network that protects organisms against cancer. It is a transcription factor that is induced upon stress signals that pose a danger to normal cell growth. Upon induction, p53 activates numerous genes and leads to cell cycle arrest or apoptosis, preventing the potential transformation into a cancer cell.[1] Around 50% of human cancers have missense point mutations in the gene for p53 that inactivate it.[2] Most of these mutations are located in the DNA-binding core domain of p53. Many of these are "structural" mutations, which thermodynamically destabilize p53, resulting in its unfolding and inactivation.[3–5] These mutations also kinetically destabilise the protein, resulting in faster unfolding rates.[6]

Different structural mutations seem to disrupt the structure of p53 core domain in different ways, ranging from local distortion to global unfolding.[3,4] It was widely believed that there is a single denatured "mutant conformation" for p53 core domain, and the specific antibody Pab240,[7] which recognises highly destabilised mutants such as R175H and V143A,[8] is directed against this "mutant form". Its target epitope includes residues 212–217 on the S7 strand, which are buried inside the hydrophobic core of the native protein and probably become exposed in these mutants.[9] Interestingly, the Pab240 epitope is in close proximity to the epitope recognised by the Pab1620 antibody, which is directed against the native structure. The Pab1620 epitope includes residues 145–157 in the loop between strands 3 and 4, and residues 201–212 in strand 6 and the loops around it.[10] Recently, the HSQC NMR spectrum of p53 core domain was assigned.[11] Based on that, chemical shift analysis of several structural p53 core domain mutants revealed some information about the structural changes in these mutants compared to the wild-type. The globally destabilised mutant

Abbreviations used: HSQC, heteronuclear single quantum coherence; ppm, parts per million; WT, wild-type.

E-mail address of the corresponding author: arf25@cam.ac.uk

V143A has global conformational changes in the β-sandwich, while mutants in loop 3 (G245S, R248Q and R249S) undergo local structural changes around the mutation site rather than global changes in the hydrophobic core.[11] However, the extent and the nature of the conformational changes of these mutants, as well as their dynamic behaviour, is yet to be established.

The loop 3 mutation R249S is one of the six "hotspots" which are the most frequent p53 mutations in cancer. This mutation is highly frequent (around 50%) in hepatocellular carcinoma in eastern Asia and sub-Saharan Africa.[12] In these cases, the R249S mutation is specifically induced by the mycotoxin aflatoxin B1, which is a major food contaminant. Aflatoxin B1 contamination has also a synergistic effect with hepatitis B virus infection.[12] The residue R249 stabilises the zinc coordination site of p53 by linking loop 3 to loop 2 *via* a salt bridge to E171 in loop 2, and stabilises loop 3 itself by forming hydrogen bonds to the backbone carbonyl groups of M246 and G245. Upon mutation to Ser, the region is destabilised by the loss of these interactions.[13] R249S is thermodynamically destabilised by 1.92 kcal/mol,[4] unfolds faster than the wild-type (WT)[6] and is unable to bind DNA.[4] The mouse p53 mutant R246S, which is the analogue of the human p53 R249S mutant, has several structural characteristics of wild-type. It interacts with the antibody Pab246, which is directed against wild-type murine p53 but not with the antibody Pab240 directed against denatured mutant p53, it binds the simian virus 40 (SV40) T-antigen and does not bind the molecular chaperone Hsp70.[14] On the other hand murine R246S does not have wild-type activity, as shown by its inability to transactivate the MCK promoter and to suppress osteosarcoma cell colony formation.[14]

Reactivation of mutant p53 is an important target in the development of therapies for cancer.[2,15] One promising strategy to reactivate destabilised p53 mutants is using a small molecule that binds the native, but not the denatured state. This would result in shift of the conformational equilibrium towards the native state leading to thermodynamic stabilisation and to restoration of activity.[5,16] We have recently reported a peptide, FL-CDB3, derived from the p53-binding protein 2 (53BP2), which binds to p53 core domain and stabilises it *in vitro*[16] and in living cells.[17]

Here, we have analysed the structural effects of the R249S mutation on the p53 core domain structure using HSQC and relaxation NMR techniques. Our results show that R249S has a folded structure, which resembles that of wild-type, with a local distortion around the mutation site and an increased flexibility of the β-sandwich. We conclude that R249S does not possess an alternative, denatured conformation, but is rather an ensemble of native and native-like conformations in a dynamic equilibrium. This implies that to rescue locally distorted mutants such as R249S, one could use a small molecule such as FL-CDB3 that binds preferentially to the native state and shifts the conformational equilibrium to the native conformation in a "chaperone" mechanism. Indeed, we show that FL-CDB3 can shift the conformation of the site distorted by the mutation in R249S towards that of wild-type.

Results

Structural effects of the R249S mutation: local distortion around the mutation site and increased flexibility in the β-sandwich

The structural effects of the R249S mutation were studied by both HSQC and relaxation NMR techniques. HSQC studies are used to indicate whether the chemical environment of the backbone amides for each residue changes upon mutation. In addition, the HSQC data can provide information about the retention or loss of secondary structure upon mutation. Relaxation methods are excellent tools to study the dynamic properties of protein backbones, and how it is affected by the mutation. Here, backbone amide ^{15}N longitudinal (R_1) and transverse (R_2) relaxation rates were used as reporters for the mobility of the p53 core domain backbone.[18] Ratios of relaxation rates, R_2/R_1, that deviate from values predicted for a structure-based model represent residues with motions that are independent from overall tumbling of the molecule. Two cases are then possible: a lower R_2/R_1 ratio for a certain residue than predicted indicates that this residue tumbles faster than the overall tumbling of the molecule due to local flexibility or unfolding; and a higher R_2/R_1 ratio than predicted indicates that the residue undergoes conformational exchange in the μs–ms time scale, which represents a dynamic equilibrium between two or more states that have different chemical environments (see Materials and Methods).

We have obtained backbone ^{15}N relaxation rates (Figures 1 and 2(a)) and HSQC two-dimensional spectra for both the wild-type and R249S core domains (Figures 2(b) and 3). The overall HSQC spectrum of R249S indicated a structured conformation that is highly similar to that of the wild-type (Figures 2(b) and 3),[11] indicating that the overall native structure is retained in R249S. The R249S mutation had two major effects on the p53 core domain structure: local distortion around the mutation site in loop 3 and increased flexibility in the β-sandwich scaffold (Figures 1 and 2). The local distortion around loop 3 was clearly indicated by the HSQC data, which showed that R249S differs from wild-type in the regions around the mutation site and the DNA-binding interface. These differences were hardly detected in the β-sandwich scaffold, and only the β-sandwich parts which are close to the DNA-binding interface were affected (Figure 2(b)).[11] Many residues around the mutation site in loop 3 could not be

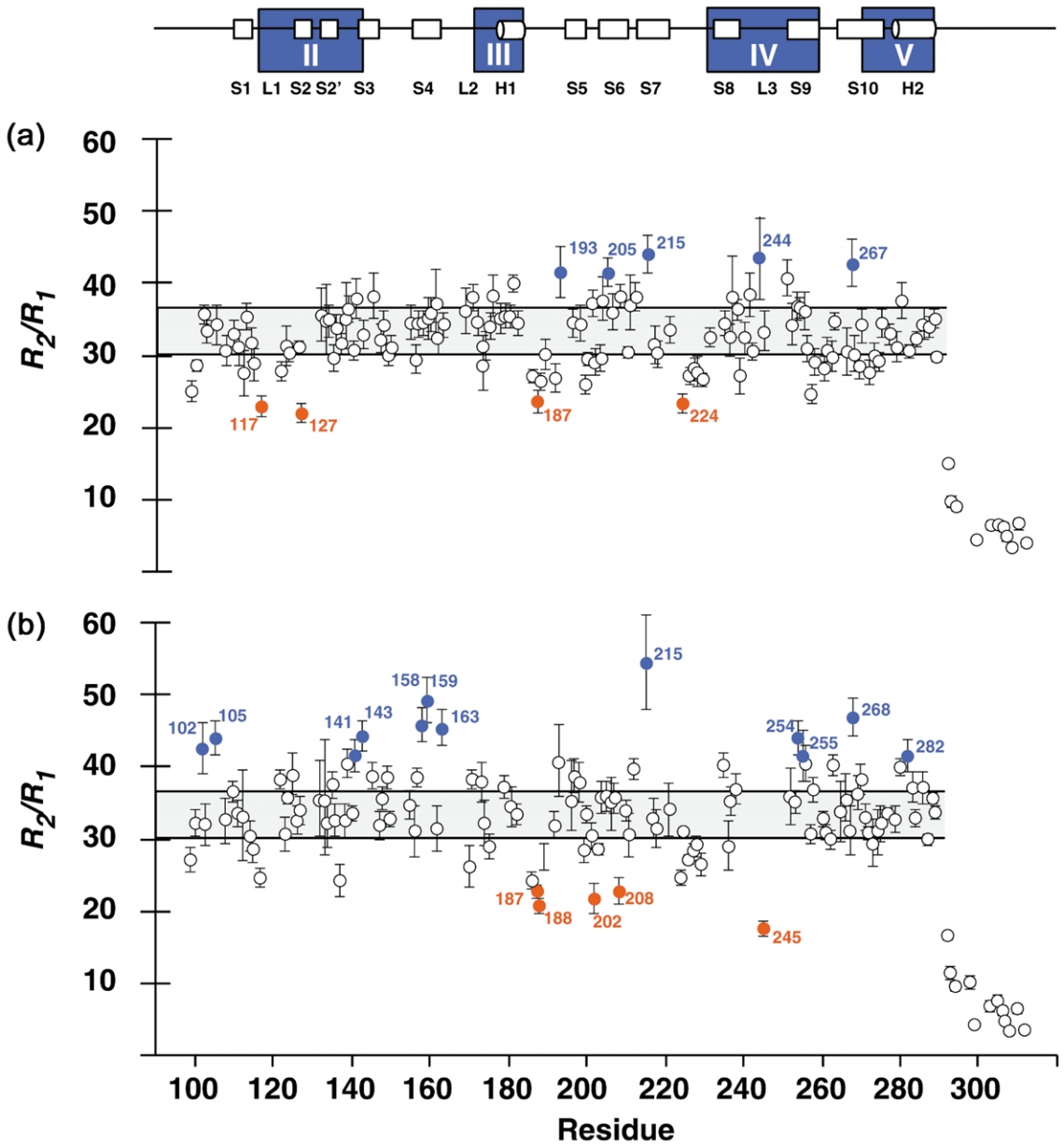

Figure 1. Dynamics of the wild-type and R249S p53 core domain. (a) R_2/R_1 relaxation ratios of the WT core domain. The grey region represents the range of values predicted for p53 as a rigid molecule (see Materials and Methods). Points in blue represent residues that deviate in a positive direction from the mean by two standard deviations and indicate areas of motion on a μs–ms time scale, which describe dynamic equilibrium between conformations. Points in red indicate residues that deviate from the mean by two standard deviations in a negative direction and indicate residues that are undergoing motions on a ps-ns time scale. (b) R_2/R_1 relaxation ratios of R249S on the same scale and labelled with the same parameters as in (a). The secondary structure of the p53 core domain with four of the five highly conserved regions boxed is shown at the top.

assigned in the R249S spectrum. This could be due to either: (1) large chemical shift differences from the wild-type values, which represent a complete change in the chemical environment of these residues; or (2) conformational equilibrium leading to exchange broadening of signals beyond detection limits. Overall, the NMR data indicated local distortion of the structure around the R249S mutation site, with retention of the native structure at the rest of the protein.

The relaxation data showed that wild-type p53 core domain had a rigid β-sandwich scaffold, while several loop regions, including those in the DNA-binding region, were dynamic (Figure 1(a)). In R249S, residues throughout the β-sandwich undergo slow (μs–ms) conformational exchange not observed in the wild-type (Figures 1 and 2(a)), indicating a looser and more flexible structure than that of wild-type (compare Figure 1(a) and (b)). However, the HSQC data showed no major differences between the wild-type and R249S in the β-sandwich region (Figure 2), indicating that

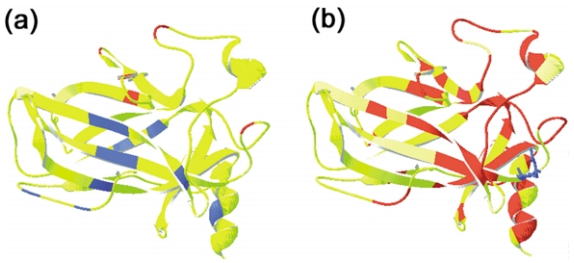

Figure 2. Structural effects of the R249S mutation on p53 core domain. (a) Dynamics analysis. Backbone dynamics data of R249S p53 core domain in solution mapped onto the p53 core domain crystal structure.[13] Residues in blue (representing reporters of slow μs–ms conformational exchange) and residues in red (representing reporters of fast ps motions) are highlighted as in Figure 1(b). (b) Chemical shift analysis. Residues in R249S, which change their chemical shift compared to the wild-type (0.125 ppm $< \Delta\partial$ for ^{15}N, 0.025 ppm $< \Delta\partial$ for ^{1}H), are colour-coded red. Residues that retain their chemical shift or those that could not be assigned are colour-coded yellow. The mutation site is colour-coded blue.

the global fold of the region remained intact in R249S. The HSQC data also ruled out the existence of a slow unfolding-refolding equilibrium between the native and a globally denatured state. Such an equilibrium would have resulted in an additional set of peaks for the unfolded state, which lacks in the R249S spectrum. Therefore, the conformational heterogeneity is likely to be caused by a dynamic equilibrium between the native structure and alternative native-like conformations.

FL-CDB3 binds wild-type and mutant p53 core domain at the same site

If the R249S mutant does indeed undergo a dynamic equilibrium, its native structure could be restored by a small molecule that binds preferentially to the native conformation and shifts the equilibrium towards the native state.[5,16] We have used HSQC NMR spectroscopy to determine whether the rationally designed p53-stabilising FL-CDB3[16] can restore the wild-type conformation to R249S (Figure 3). As a comparison, we have studied the effect of FL-CDB3 on the DNA contact mutant R273H, which is in a native conformation and not in a dynamic equilibrium.[4,11] Changes in the chemical shifts of p53 core domain backbone amides (^{1}H and ^{15}N) were measured and used to identify the structural effects generated upon FL-CDB3 binding (Figures 3 and 4). In principle, such chemical shift changes are observed for residues that either bind a ligand directly, or change their conformation due to long-range effects.

The spectra of wild-type and mutant p53 were similar to each other and in agreement with previous studies.[11] Upon FL-CDB3 binding, peaks

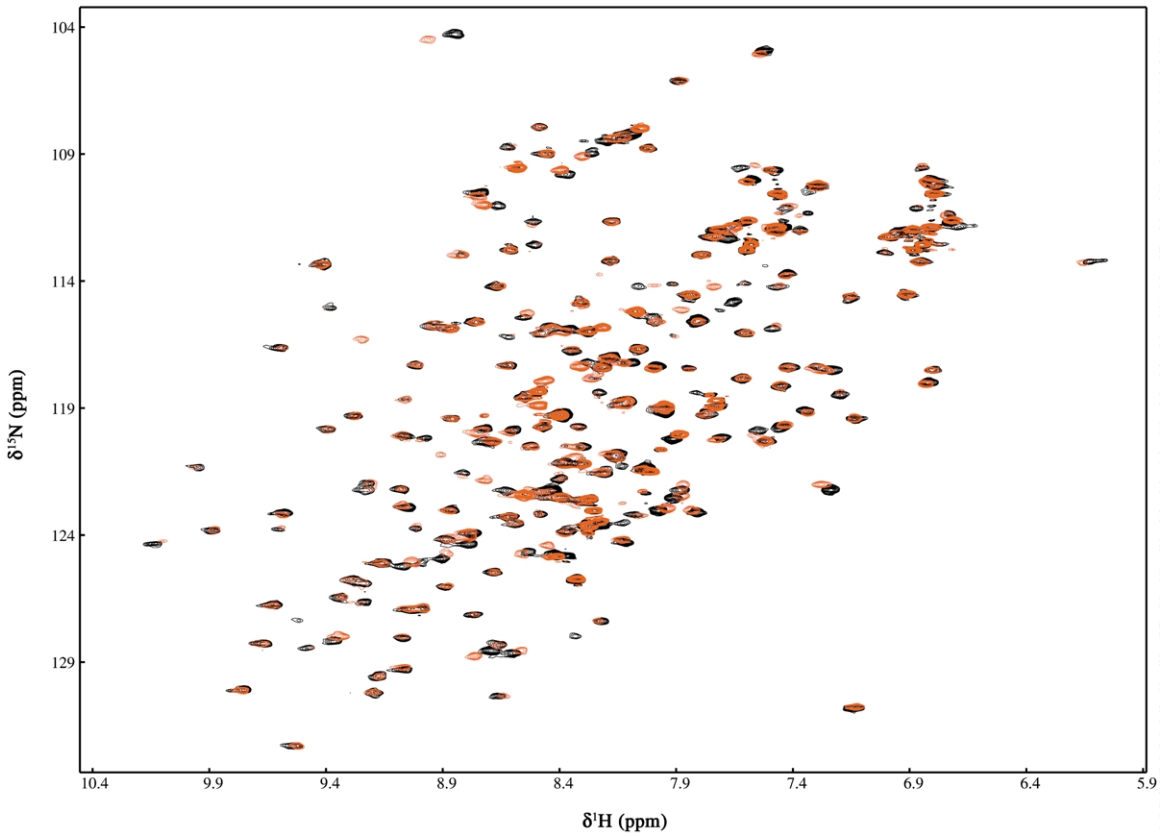

Figure 3. NMR HSQC spectra of R249S p53 core in the presence of FL-CDB3. Black, R249S (150 μM); red, R249S (150 μM) in the presence of 600 μM FL-CDB3 (for peak assignment see Wong *et al.*[11]).

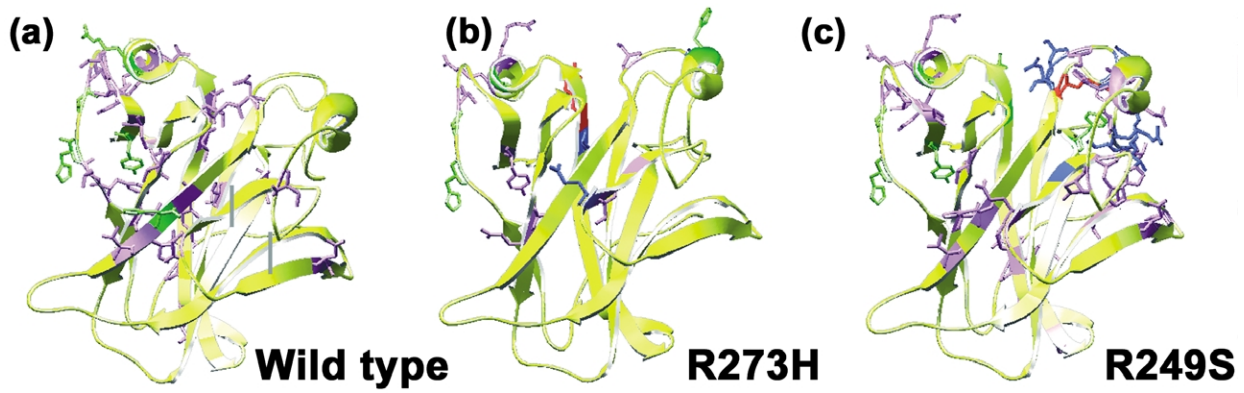

Figure 4. Chemical shift changes (Δ∂) in p53 core domain wild-type and mutants upon binding to FL-CDB3: (a) wild-type, (b) R273H, (c) R249S. Deviations above five times the standard deviation ($\Delta\partial > 0.25$ ppm for ^{15}N and $\Delta\partial > 0.05$ ppm for ^{1}H) were considered significant (colour-coded green). Δ∂ differences between 2.5 times and five times the standard deviation ($0.125 < \Delta\partial < 0.25$ ppm for ^{15}N, $0.025 < \Delta\partial < 0.05$ ppm for ^{1}H) were considered as medium (colour-coded purple), and Δ∂ differences below 2.5 times the standard deviation ($\Delta\partial < 0.125$ ppm for ^{15}N and $\Delta\partial < 0.025$ ppm for ^{1}H) were considered insignificant (colour-coded yellow). See the text for residue number details. Residues that disappeared in the mutant spectrum compared to the wild-type are colour-coded blue. The mutation sites are colour-coded red. The p53 core domain coordinates were taken from Cho *et al*.[13] Picture was generated using swissPDB viewer.[22] Spectra for wild-type and R249S were taken at 20 °C. The R273H spectrum was taken at 25 °C. The buffer was 25 mM phosphate (pH 7.2), 150 mM KCl, 5 mM DTT, 2% (v/v) $^{2}H_2O$.

corresponding to the backbone of different types of residues behaved differently (Figures 3 and 4). (1) Residues with changes in chemical shifts upon peptide binding both in wild-type and mutant p53 (e.g. F113, L114, H115, G117, T118, S121 and V122 from loop 1) are directly involved in peptide binding and form the peptide-binding site, which is the same in wild-type, R249S and R273H (Figure 4). (2) Residues with no detectable chemical shift changes on peptide binding were mainly in the β-sandwich. (3) Residues, where there were changes in chemical shift upon FL-CDB3 binding in only the R249S mutant but not in wild-type p53, are not in the peptide-binding site (see below). FL-CDB3 bound p53 core wild-type and both the R249S and R273H mutants at the same site. This is a well-defined site including loop 1, helix 2 and strand 8, and overlapping the binding site of the non-labelled CDB3,[16] indicating that labelling does not change the binding site (Figure 4). Binding of FL-CDB3 was concentration-dependent, and larger chemical shift changes were observed with eightfold excess of the peptide compared to fourfold excess (data not shown).

FL-CDB3 shifted the conformational equilibrium of R249S towards the native state

To test whether upon binding R249S, FL-CDB3 can shift its conformational equilibrium towards the native state, we have used HSQC NMR which is indicative of the chemical environment of the backbone amide for each residue. We have asked the following questions. First, does FL-CDB3 binding affect the chemical shifts of residues outside the peptide binding-site in R249S? If so, FL-CDB3 binding is likely to trigger a long-range conformational effect in R249S. Second, for the same residues, does FL-CDB3 binding decrease the chemical shift difference between R249S and the wild-type? If so, then the chemical environment of these residues becomes more native-like upon FL-CDB3 binding, meaning a shift of the conformational equilibrium towards the wild-type.

Chemical shift changes in R249S upon FL-CDB3 binding were found at the site distorted by the mutation, which is remote from the peptide-binding site and situated at the other side of the DNA-binding interface (Figures 3 and 4(c)). Specifically, these chemical shift changes were found in the loop 2 and helix 1 region (residues shifted included Y163, H168, T170, C176, E180 and H193); the loop between strand 6 and strand 7 (D208, T211, F212, R213 and S215); and residues T256 and E258 from strand 9 and G266 from strand 10. Chemical shift changes in these regions upon peptide binding were not seen for the wild-type or for the R273H contact mutant. This is expected, as these two proteins possess a native structure and do not undergo a dynamic conformational equilibrium. The possibility that these chemical shift changes in R249S are due to a second binding site of the peptide can be excluded, since the R249S-FL-CDB3 binding stoichiometry is 1:1.[16] Thus, these chemical shift changes result from a long-range conformational effect of FL-CDB3 binding.

To determine whether the FL-CDB3-induced shift of the R249S conformational equilibrium at the regions described above is towards the native conformation, we measured the change in the chemical shift difference between wild-type and R249S for each residue upon FL-CDB3 binding. If, for the above-mentioned residues, the chemical shifts of the wild-type and R249S became closer in presence of the peptide, it means that their chemical environments became similar. The absolute

value of the difference between the wild-type-R249S chemical shift differences without and with FL-CDB3 was defined as ΔΔδ, and is shown in Figure 5. For regions outside the peptide-binding site, where there was no effect of FL-CDB3 on the chemical shift of the wild-type, a high ΔΔδ value for R249S implied that the peptide shifted the R249S conformational equilibrium. In the same protein regions, ΔΔδ values within the noise level meant that the chemical shift distance from the wild-type and thus the conformational equilibrium of the particular residue were not affected by the peptide. We have identified high ΔΔδ values at several sites in R249S: the peptide-binding site in loop 1 and helix 2, the mutation site around loop 3 and sites within loop 2, helix 1 and strands 6 and 7. The latter sites include the residues for which the peptide changed the R249S chemical shift by a long-range effect as described above (Figure 4(c)).

Figure 6 is a close-up of the chemical shift changes for the residues described above, which were shifted in R249S but not in the wild-type. These residues are outside the FL-CDB3-binding site, but their chemical shifts changed on FL-CDB3 binding and they possessed high ΔΔδ values. The chemical shifts of the loop 2 and helix 1 residues T170, C176, E180 and H193 (Figure 6(a)), changed in presence of FL-CDB3 from their original values (representing the distorted conformation, in red) to the positions marked green, which were closer to these of wild-type (black) and wild-type + FL-CDB3 (blue). The wild-type (black) was almost not affected by the peptide (blue). The same trend, but with weaker changes, was also observed for the residues in the loop between strand 6 and strand 7 (Figure 6(c); same colour code). The residues whose conformation was shifted towards wild-type (colour-coded red in Figure 6(b) and (d)) were remote from the peptide-binding site (colour coded green in Figure 6(b) and (d)). Many residues in the mutation and distortion site underwent large chemical shift changes from wild-type to R249S (colour coded blue in Figure 4) and their peaks in the R249S spectrum could not be assigned (labelled as $\Delta\Delta\delta = 0$ in Figure 5). However, since these residues are located in the distortion site in close proximity to the residues whose conformation was restored by FL-CDB3, we believe that FL-CDB3 is able to restore the conformation of these residues as well. In summary, FL-CDB3 shifted the conformation of the distorted mutant R249S towards the wild-type by binding at one side of

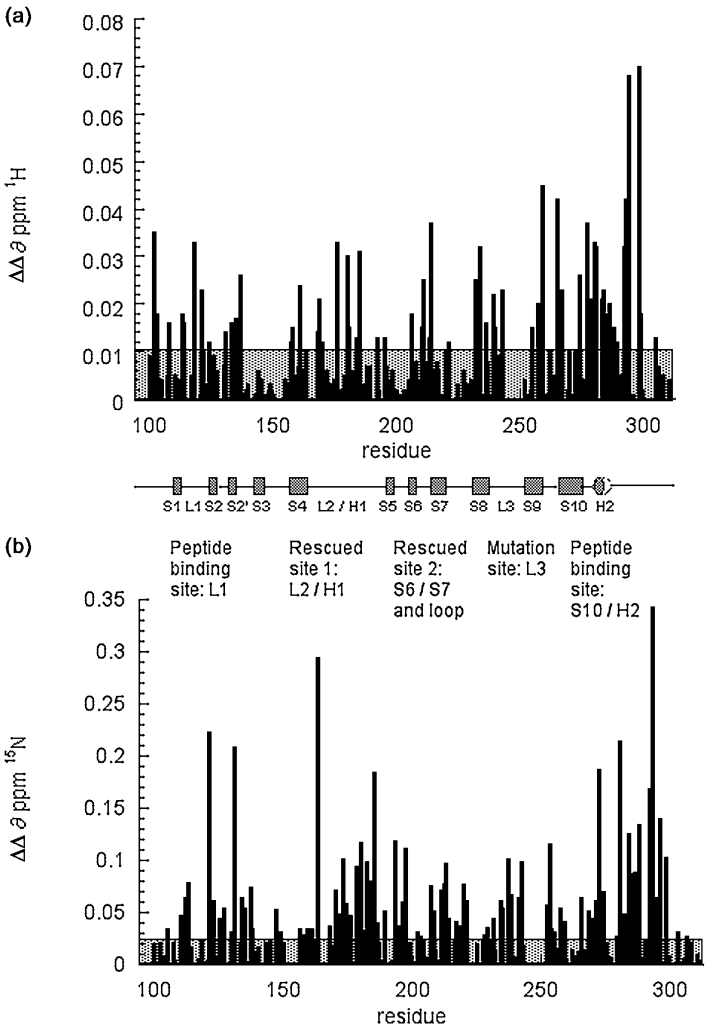

Figure 5. FL-CDB3 reverts the chemical shifts of distorted regions in R249S towards wild-type. The ability of FL-CDB3 to revert the structural effects of the R249S mutation was measured by comparing the chemical shift difference between wild-type and R249S in the presence and the absence of the peptide. The bar graph shows the difference between the WT–R249S chemical shift differences (Δδ) without and with FL-CDB3, which can be described as:

$$\Delta\Delta\delta = \mathrm{Abs}\{\Delta\delta[\mathrm{WT\text{-}R249S}] - \Delta\delta[(\mathrm{WT} + \mathrm{FL\text{-}CDB3}) - (\mathrm{R249S} + \mathrm{FL\text{-}CDB3})]\}$$

for the ^{1}H (a) and ^{15}N (b) chemical shifts for each residue. For regions outside the peptide-binding site, the high bars indicate residues in R249S for which the chemical shifts have moved back towards the wild-type position. For these residues, the wild-type and R249S chemical shifts in the presence of the peptide are much closer than in its absence. Low bars mean that upon peptide binding, the particular residue in R249S does not significantly change its chemical shift. The grey box represents the baseline.

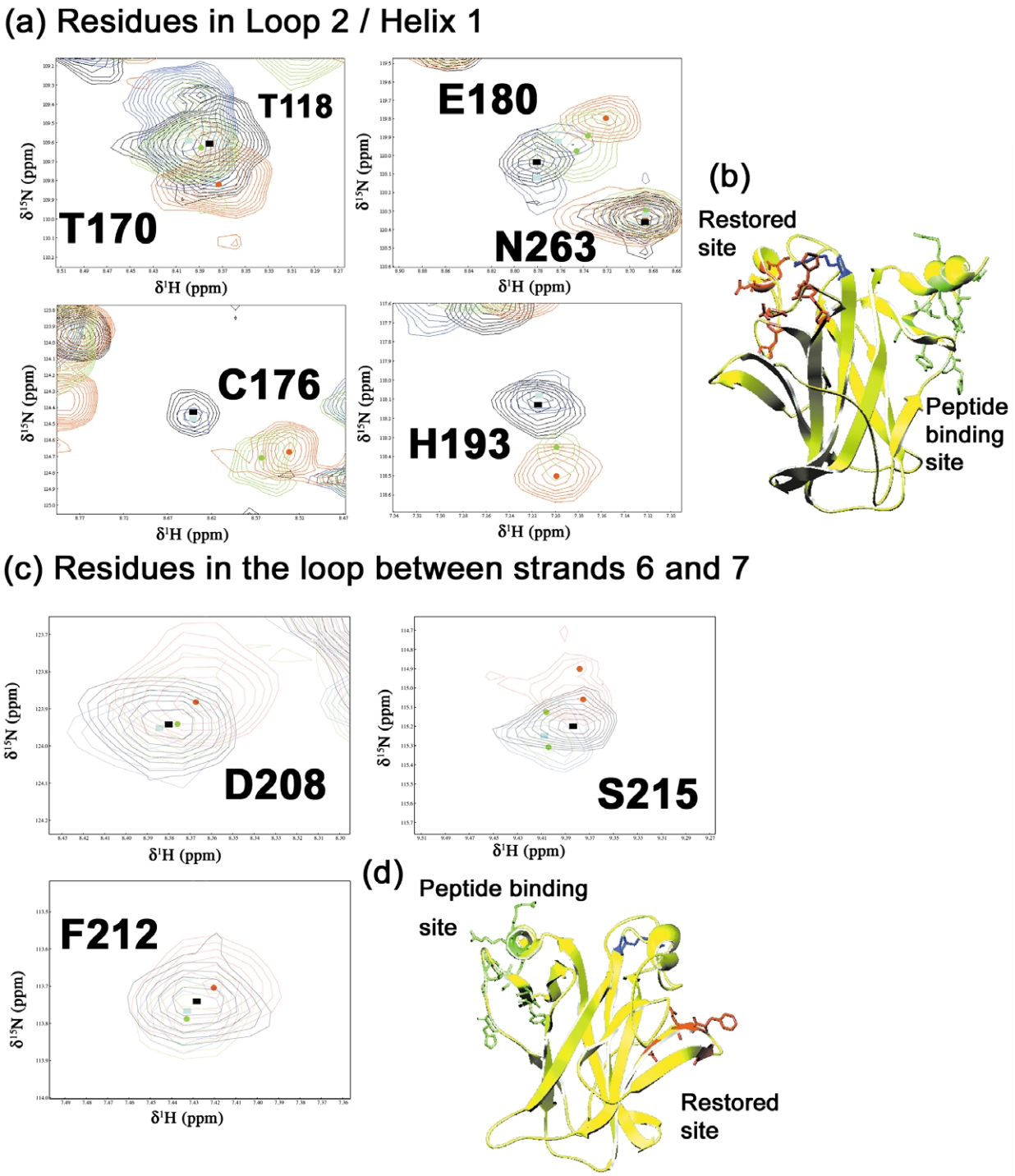

Figure 6. Residues in R249S whose chemical shifts are shifted towards wild-type values upon binding of FL-CDB3. (a) Chemical shift changes in representative residues in the loop 2/helix 1 region: T170, E180 C176, and H193. Black, wild-type p53 core (150 μM); blue, wild-type p53 core (150 μM) in the presence of 600 μM FL-CDB3; red, R249S (150 μM); green, R249S (150 μM) in the presence of 600 μM FL-CDB3. The rectangles and circles (same colour code) represent the maximum for each peak. Note that N263 is not affected by peptide binding and by the mutation. (b) Mapping of (a) on the p53 core domain structure: red, residues in the loop 2/helix 1 region of R249S shifted towards wild-type conformation; green, FL-CDB3 binding residues; blue, mutation site. For clarity, the p53 core domain is viewed from the opposite side compared to Figure 4. (c) Chemical shift changes in representative residues in the loop between strands 6 and 7: D208, S215 F212. Black, wild-type p53 core (150 μM); blue, wild-type p53 core (150 μM) in the presence of 600 μM FL-CDB3; red, R249S (150 μM); green, R249S (150 μM) in the presence of 600 μM FL-CDB3. The rectangles and circles (same colour code) represent the maximum for each peak. (d) Mapping of (c) on the p53 core structure: red, residues in the loop between strands 6 and 7 of R249S shifted towards wild-type conformation; green, FL-CDB3 binding residues; blue, mutation site.

the protein and having a long-range conformational effect on the distortion site at the other side of the protein.

Discussion

Dynamic conformational equilibrium of R249S

Using a combination of HSQC and relaxation NMR techniques, we were able to provide insight into the conformation of a hot-spot p53 mutant. Overall, R249S has a folded native-like structure. There are two major structural effects of the R249S mutation: the site of mutation is distorted, with the local distortion spreading throughout the DNA-binding interface; and the β-sandwich retains the wild-type structure, but its flexibility is increased relative to wild-type. There is no structural difference between R249S and the wild-type in this region, and thus this increased flexibility is most likely to be caused by a dynamic equilibrium between the native structure and several alternative native-like conformations. We conclude that R249S does not adopt a single unfolded mutant conformation. Our findings are consistent with the antibody-based studies, which show that the murine analogue of R249S interacts with antibody against the native but not against the denatured state.[14] The key residues in the Pab246 epitope are residues 202–204,[10] which are at the loop between strands 5 and 6 and the beginning of strand 6. The conformation of these residues is not affected by the R249S mutation, explaining the binding of the antibody to the same epitope in R249S. The increased flexibility of the β-sandwich does not lead to a profound structural change that would result in loss of binding to Pab246 or to exposure of the Pab240 epitope (residues 212–217). The lack of binding to Pab240 is also consistent with our observation that no predominantly denatured state is populated within the R249S conformational equilibrium.

A partial conformational rescue of the distorted site in R249S was found for the suppressor mutant H168R.[19] The conformation of residues in the loop 2 region is also partly restored. The mechanism, however, is different. The rescue by the suppressor mutation H168R results from a direct effect of the arginine residue introduced at position 168, which compensates for the loss of the arginine at position 249, whereas FL-CDB3 acts by inducing a conformational change and not by a direct contact with the mutation site. Interestingly, H168 is one of the residues whose conformation is partly restored by FL-CDB3.

Implications of the dynamic equilibrium

As the conformational equilibrium of R249S is dynamic and includes the native structure, any molecule that binds specifically to the native structure and not alternate conformations will shift the equilibrium back to wild-type.[5] Indeed, we found that FL-CDB3 is able to bind R249S and shift the conformation of its distorted DNA-binding interface *via* long-range effects. This implies that, in general, distorted p53 mutants could be rescued by drugs that bind outside the distortion site.

In principle, the binding of a genuine ligand of p53, e.g. a promoter or a p53-binding protein will also perturb the equilibrium to favour wild-type structure. The effect of the equilibrium is to lower the affinity of the mutant protein for its substrates because only a fraction of the population is in the correct structure. This has implications for the use of drugs like FL-CDB3 in a chaperone strategy that rescues unstable mutants. If the drug and a natural ligand compete for the same binding site, then the role of the drug will be to bind to the destabilised mutant immediately on its biosynthesis and stop it from denaturing before it is transported to a location where the natural ligand can bind.[6] If, on the other hand, the drug and the ligand bind to separate sites, then the drug and the ligand will bind synergistically, since both bind to the same conformation. Accordingly, the drug will both stabilize the mutant and improve affinity. FL-CDB3 is thus a prototype for the first strategy.

The presence of a dynamic equilibrium also affects the analysis of data obtained from antibodies that are directed against either the native or highly denatured states. Suppose that there is a dynamic equilibrium between such states, as could be the case for the more destabilised mutants, especially the β-sandwich ones. Then, binding of an antibody such as Pab240 to the denatured state will shift the equilibrium towards the denatured state. This could result in unfolding of the whole protein and high binding to Pab240, although the protein might not be 100% unfolded in its absence. Given that we have shown the structure of R249S is a distorted version of wild-type p53 core domain, and that other mutants have various degrees of structural changes[11] or are highly denatured at body temperature,[4,6] it is unlikely that there is a single mutant conformation of p53.

Materials and Methods

Peptide synthesis

The peptides were synthesised using a Pioneer peptide synthesizer (Perseptive) using standard Fmoc chemistry. Fluorescein was coupled to the N terminus of the peptides on the Pioneer peptide synthesizer using fourfold excess of Fluorescein-Osu (molecular probes) and fourfold excess of HoBt. The peptides were purified and characterised as described.[16]

Protein expression and purification

Human p53 core wild-type and mutants (residues 94–312) were cloned, expressed and purified as described.[3]

^{15}N-labelled human p53 core was produced as described.[11]

HSQC NMR spectroscopy

All ^{1}H, ^{15}N-HSQC spectra were acquired at various temperatures on a Bruker DRX 600 MHz spectrometer as described.[11] Samples for NMR experiments contained ^{15}N-labelled wild-type or mutant p53 core at a concentration of 150 μM and FL-CDB3 at a concentration of 600 μM or 1.2 mM. The buffer was 150 mM KCl, 5 mM dithiothreitol (DTT), 2% $^{2}H_2O$ in 25 mM sodium phosphate (pH 7.2). Chemical shift analysis was performed as described.[16]

Dynamics analysis by NMR

Backbone amide ^{15}N longitudinal (R_1) and transverse (R_2) relaxation rates were used as reporters for the mobility of the p53 core domain main-chain.[18] In the ideal case of a rigid spherical protein, the R_2/R_1 ratios should be constant for all residues. In the case of anisotropic tumbling, however, R_2/R_1 ratios may vary dependent on the orientation of NH vectors with respect to the diffusion tensors of the protein. Therefore, relaxation data were analysed in the context of an axial symmetry model (compared to a full asymmetric model, statistical analysis showed that the tumbling of p53 core domain is better described by an axial symmetry model). Fitting of relaxation data to diffusion models was carried out with the program QUADRIC DIFFUSION (from Professor A. Palmer, University of Columbia), which uses the local diffusion approximation.[20,21] To avoid inclusion of relaxation data that may be affected by large amplitude internal motion or substantial conformational exchange, the diffusion parameters were derived using only R_2/R_1 ratios of residues in secondary structure elements (similar results were obtained when only R_2/R_1 ratios within 1.5 standard deviations from mean were included). The anisotropy (Dpar/Dper ratio) determined for p53 core domain was 1.22 (Dpar/Dper = 1 in the case of isotropic tumbling) and the effective correlation time was 18.1 ns. Based on this diffusion model, R_2/R_1 ratios were predicted to range from 30, for NH vectors that are perpendicular to the symmetry axis, to 37, for those parallel with the axis. The predicted range of R_2/R_1 ratios is indicated as a grey area in Figure 1.

Standard pulse sequences were used to measure longitudinal (R_1) and transverse (R_2) relaxation rates on a Bruker DRX-600 spectrometer. The R_1 relaxation times were set to 40, 80, 160, 320, 480, 640, 960 ms, and 1.2, 1.6 and 2.0 seconds. R_2 experiments were acquired with relaxation times of 7, 14, 21, 28, 42, 56, 84, 112, 168 and 210 ms. Each time point was repeated three times and averaged for the final analysis. Peak intensities were fitted to monoexponential equations in KaleidaGraph 3.0 (Abelbeck Software) to obtain R_1 and R_2. The uncertainties of the R_1 and R_2 rates were estimated from the fitting routine.

Acknowledgements

This work was supported by Cancer Research UK and the MRC. A.F. was supported by a long-term fellowship (no. LT00056/2000-M) from the Human Frontier Science Program. We thank Mark Bycroft for helpful discussions and advice and Karoly von Glos for peptide synthesis. S.R. was supported by a Marie Curie Fellowship from the EU.

References

1. Vousden, K. H. & Lu, X. (2002). Live or let die: the cell's response to p53. *Nature Rev. Cancer*, **2**, 594–604.
2. Lane, D. P. & Hupp, T. R. (2003). Drug discovery and p53. *Drug Discov. Today*, **8**, 347–355.
3. Bullock, A. N., Henckel, J., DeDecker, B. S., Johnson, C. M., Nikolova, P. V., Proctor, M. R. *et al.* (1997). Thermodynamic stability of wild-type and mutant p53 core domain. *Proc. Natl Acad. Sci. USA*, **94**, 14338–14342.
4. Bullock, A. N., Henckel, J. & Fersht, A. R. (2000). Quantitative analysis of residual folding and DNA binding in mutant p53 core domain: definition of mutant states for rescue in cancer therapy. *Oncogene*, **19**, 1245–1256.
5. Bullock, A. N. & Fersht, A. R. (2001). Rescuing the function of mutant p53. *Nature Cancer Rev.* **1**, 68–76.
6. Friedler, A., Veprintsev, D. B., Hansson, L. O. & Fersht, A. R. (2003). Kinetic instability of p53 core domain mutants: implications for rescue by small molecules. *J. Biol. Chem.* **278**, 24108–24112.
7. Gannon, J. V., Greaves, R., Iggo, R. & Lane, D. P. (1990). Activating mutations in p53 produce a common conformational effect. A monoclonal antibody specific for the mutant form. *EMBO J.* **9**, 1595–1602.
8. Legros, Y., Meyer, A., Ory, K. & Soussi, T. (1994). Mutations in p53 produce a common conformational effect that can be detected with a panel of monoclonal antibodies directed toward the central part of the p53 protein. *Oncogene*, **9**, 3689–3694.
9. Stephen, C. W. & Lane, D. P. (1992). Mutant conformation of p53. Precise epitope mapping using a filamentous phage epitope library. *J. Mol. Biol.* **225**, 577–583.
10. Wang, P. L., Sait, F. & Winter, G. (2001). The "wild-type" conformation of p53: epitope mapping using hybrid proteins. *Oncogene*, **20**, 2318–2324.
11. Wong, K. B., DeDecker, B. S., Freund, S. M., Proctor, M. R., Bycroft, M. & Fersht, A. R. (1999). Hot-spot mutants of p53 core domain evince characteristic local structural changes. *Proc. Natl Acad. Sci. USA*, **96**, 8438–8442.
12. Aguilar, F., Hussain, S. P. & Cerutti, P. (1993). Aflatoxin B1 induces the transversion of G → T in codon 249 of the p53 tumor suppressor gene in human hepatocytes. *Proc. Natl Acad. Sci. USA*, **90**, 8586–8590.
13. Cho, Y., Gorina, S., Jeffrey, P. D. & Pavletich, N. P. (1994). Crystal structure of a p53 tumor suppressor–DNA complex: understanding tumorigenic mutations. *Science*, **265**, 346–355.
14. Ghebranious, N., Knoll, B. J., Wu, H., Lozano, G. & Sell, S. (1995). Characterization of a murine p53ser246 mutant equivalent to the human p53ser249 associated with hepatocellular carcinoma and aflatoxin exposure. *Mol. Carcinog.* **13**, 104–111.

15. Lane, D. P. & Lain, S. (2002). Therapeutic exploitation of the p53 pathway. *Trends Mol. Med.* **8**, S38–S42.
16. Friedler, A., Hansson, L. O., Veprintsev, D. B., Freund, S. M., Rippin, T. M., Nikolova, P. V. *et al.* (2002). A peptide that binds and stabilizes p53 core domain: chaperone strategy for rescue of oncogenic mutants. *Proc. Natl Acad. Sci. USA*, **99**, 937–942.
17. Issaeva, N., Friedler, A., Bozko, P., Wiman, K. G., Fersht, A. R. & Selivanova, G. (2003). Rescue of mutants of the tumour suppressor p53 in cancer cells by a designed peptide. *Proc. Natl Acad. Sci. USA*, **100**, 13303–13307.
18. Kay, L. E., Torchia, D. A. & Bax, A. (1989). Backbone dynamics of proteins as studied by ^{15}N inverse detected heteronuclear NMR spectroscopy: application to staphylococcal nuclease. *Biochemistry,* **28**, 8972–8979.
19. Nikolova, P. V., Wong, K. B., DeDecker, B., Henckel, J. & Fersht, A. R. (2000). Mechanism of rescue of common p53 cancer mutations by second-site suppressor mutations. *EMBO J.* **19**, 370–378.
20. Lee, L. K., Rance, M., Chazin, W. J. & Palmer, A. G., III (1997). Rotational diffusion anisotropy of proteins from simultaneous analysis of ^{15}N and ^{13}C alpha nuclear spin relaxation. *J. Biomol. NMR*, **9**, 287–298.
21. Bruschweiler, R., Liao, X. & Wright, P. E. (1995). Long-range motional restrictions in a multidomain zinc-finger protein from anisotropic tumbling. *Science*, **268**, 886–889.
22. Guex, N. & Peitsch, M. C. (1997). SWISS-MODEL and the Swiss-PdbViewer: an environment for comparative protein modeling. *Electrophoresis*, **18**, 2714–2723.

Edited by J. Karn

(Received 3 October 2003; received in revised form 27 November 2003; accepted 2 December 2003)